Chinese Chemical Letters 32 (2021) 3105–3108

Contents lists available at ScienceDirect

Chinese Chemical Letters

journal homepage: www.elsevier.com/locate/cclet

Communication

Water molecule-induced hydrogen bonding between cellulose nanofibers toward highly strong and tough materials from wood aerogel

Xiaoshuai Han[a], Zhenxing Wang[b], Linhu Ding[a], Lian Chen[a], Feng Wang[a], Junwen Pu[b], Shaohua Jiang[a,*]

[a] Co-Innovation Center of Efficient Processing and Utilization of Forest Resources, College of Materials Science and Engineering, Nanjing Forestry University, Nanjing 210037, China
[b] MOE Engineering Research Center of Forestry Biomass Materials and Bioenergy, Beijing Forestry University, Beijing 100083, China

ARTICLE INFO

Article history:
Received 15 February 2021
Received in revised form 13 March 2021
Accepted 17 March 2021
Available online 19 March 2021

Keywords:
Wood aerogel
Cellulose nanofibers
Water molecules
Hydrogen bonding
Strength and toughness

ABSTRACT

Lightweight, highly strong and bio-based structural materials remain a long-lasting challenge. Here, inspired by nacre, a lightweight and high mechanical performance cellulosic material was fabricated via a facile and effective top-down approach and the resulting material has a high tensile strength of 149.21 MPa and toughness of 1.91 MJ/m^3. More specifically, the natural balsawood (NW) was subjected to a simple chemical treatment, removing most lignin and partial hemicellulose, follow by freeze-drying, forming wood aerogel (WA). The delignification process produced many pores and exposed numerous aligned cellulose nanofibers. Afterwards, the WA absorbed a quantity of moisture and was directly densified to form above high-performance cellulosic material. Such treatment imitates highly ordered "brick-and-mortar" arrangement of nacre, in which water molecules plays the role of mortar and cellulose nanofibrils make the brick part. The lightweight and good mechanical properties make this material promising for new energy car, aerospace, *etc*. This paper also explains the strengthening mechanism for making biomimetic materials by water molecules-induced hydrogen bonding and will open a new path for designing high-performance bio-based structural materials.

Materials that have lightweight, high strength and good toughness properties are attracting more attention because of their promising applications for architecture, new energy vehicles, aerospace, etc. However, the mechanical properties of strength and toughness are often mutually exclusive [1]. Surprisingly, nature gives us some inspirations to fabricate strong yet tough materials, and the nacre is a good example. The nacre is a kind of material possessing excellent strength and toughness attributing to highly ordered "brick-and-mortar" arrangement and robust interfacial bonding [2,3]. Inspired by nacre, scientists assembled a series of high-performance materials, including Chitosan-Montmorillonite nacre-like film [4], clay-based nacre-like composites [5,6], graphene oxide-based artificial nacres [7], bulk artificial nacres [8], lignocellulose-based artificial nacre [9,10], *etc*. However, there are many shortcomings in above assembling technique, such as chemical intensive, energy consuming, small scale, and complicated forming process.

Wood is a kind of biomass material and it is abundant, renewable, and sustainable in nature [11–16]. When it comes to high-performance structural materials, we should first think of the use of wood and its derivatives. Nanocellulose is a nanoscale semi-crystalline derivative of cellulose [17–20]. Nanocellulose has many good physical and mechanical properties, such as low density (1.6 g/cm^3), high tensile strength (0.3–1.4 GPa) and excellent stiffness (140 GPa), making it a desirable reinforced material [21–23]. Researchers have already used the nanocellulose to fabricate a series of strong and tough nacre-mimic materials, such as nanopapers [24], functional composite paper and films [25,26], three-dimensional transparent composites [27], *etc*. Although the Nanocellulose-based strengthening and toughening materials are attractive, the extraction of nanocellulose is tedious and chemical/energy intensive. In recent years, some high strong wood-based structural materials (such as transparent wood composites [28,29]) are manufactured using top-down method, to evade the intricate nanocellulose extraction process and maintain

* Corresponding author.
E-mail address: shaohua.jiang@njfu.edu.cn (S. Jiang).

https://doi.org/10.1016/j.cclet.2021.03.044

nanocellulose groups' well-aligned structure. But the adding of resin makes the resulting products become not pure "green" and sustainable. So, finding a wood "glue" with natural, "green", good adhesive properties, directly used is in demand and valuable.

Recently, water-induced hydrogen bonding assembly strategy is widely used to fabricate functional polymeric materials. Water molecules as co-monomers/structural water were involved in polymers and they played a big role in tuning mechanical properties of graphene oxide paper [30] and improving adhesion of supramolecular [31]. In addition to the application in fossil-based materials, it was also found that water molecules could change the tensile strength of cellulose bulk materials [32] and simultaneously improve the strengthening and toughening of cellulose-based materials [20,33].

Herein, we try to fabricate a lightweight and strong cellulosic material by means of water molecules-induced hydrogen-bonding between cellulose nanofibers as shown in Fig. 1. It is a top-down approach for fabricating high-performance cellulosic materials through compressing rehydrated wood aerogel (WA). In detail, natural balsawood (NW) was successively delignified and freeze-dried forming WA with well-aligned cellulose nanofibers. Next, the oven-dried WAs absorbed a certain amount of water molecules, followed by directly compressed at room temperature. Finally, the compressed samples were dried at 70 °C to be the high-performance cellulosic materials (The materials, chemicals, preparation process and characterization can be found in Supporting information). The delignification process can expose more cellulose nanofibrils within the wood cell walls; Absorbing water molecules can soft the cellulose nanofibrils, tending to entangle nanofibrils under compression. These two critical steps enabled superior mechanical performance of the high-performance structural materials.

Lignin is hydrophobic and it will hinder the investigation of water molecules effect on forming hydrogen bonding between cellulose nanofibers. So, we conduct the delignification using sodium chlorite ($NaClO_2$). The result of delignification showed the delignified wood (DW) was composed of 77.72% cellulose, 16.78% hemicellulose, and 2.68% lignin, demonstrating 4.30% hemicellulose and 88.92% lignin removal (Fig. 2a). In order to further validate the delignification effect, the NW and DW were characterized by FTIR spectroscopy (Figs. 2c and d). For NW, there are characteristic lignin absorption peaks at 1508 cm^{-1} and 1595 cm^{-1} (C=H stretching of the aromatic rings), 1365 cm^{-1} (symmetric C—H bending from methoxyl group), and 1233 cm^{-1} (C—O stretching of the aromatic rings). Meanwhile, the absorption peak at 1734 cm^{-1} belongs to unconjugated carbonyl C=O in hemicellulose. After

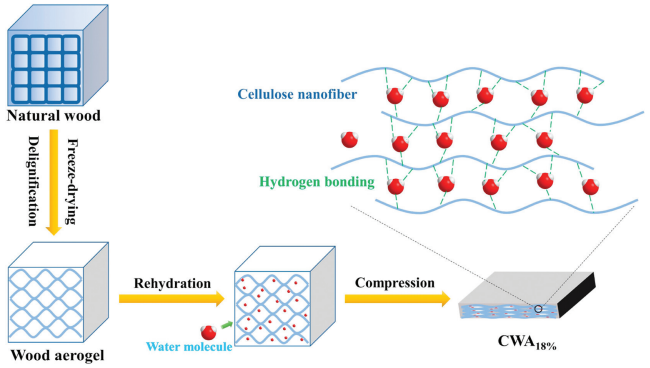

Fig. 1. Schematic illustration of the top-down fabrication of lightweight high-performance cellulosic material. During this process, the natural balsawood (NW) was converted into wood aerogel (WA) by delignification and freeze-drying, and then WA went through rehydration and compression under different moisture contents to form final product.

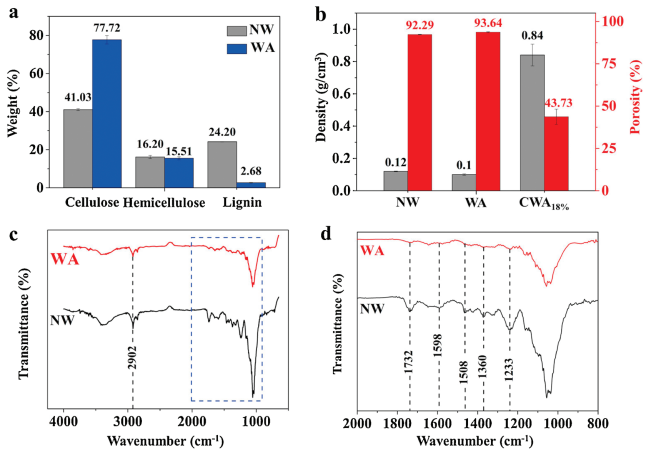

Fig. 2. (a) Composition analysis of the natural wood (NW) and the wood aerogel (WA). (b) Density and porosity of NW, WA and compressed wood aerogel (CWA) compressed under 18% moisture content ($CWA_{18\%}$). (c, d) FTIR spectra of NW and WA.

delignification process, above typical absorption peaks for lignin and hemicellulose disappeared. During sample preparation, the wet DW was freeze-dried into WA. In the freeze-drying process, the DW swelled by ice crystals. Therefore, WA showed the lowest density of 0.10 g/cm^3 and highest porosity (93.64%) (Fig. 2b). Before compression, the oven-dried WA was conditioned in a desiccator providing 97.6% ± 0.5% relative humidity (RH). Cellulose nanofiber is a kind of hygroscopic material, tending to attracting water through hydrogen bonding *via* its surface O and H atoms. After absorbing different moisture, the WAs were then compressed. At 0% moisture content (MC), the WA is hard to be compressed due to sponge-like structure. With the increase of MC, The WA was more likely to be compressed into dense and compact material because of forming some hydrogen bonding between cellulose nanofibers. The density of WA compressed at 18% moisture content ($CWA_{18\%}$) was 0.84 g/cm^3, which is more than 8 times that for WA. Therefore, the $CWA_{18\%}$ had a lowest porosity (43.73%).

The morphology and structure of the NW, WA and $CWA_{18\%}$ were shown in Fig. 3. Figs. 3a and b showed the light brown NW turns

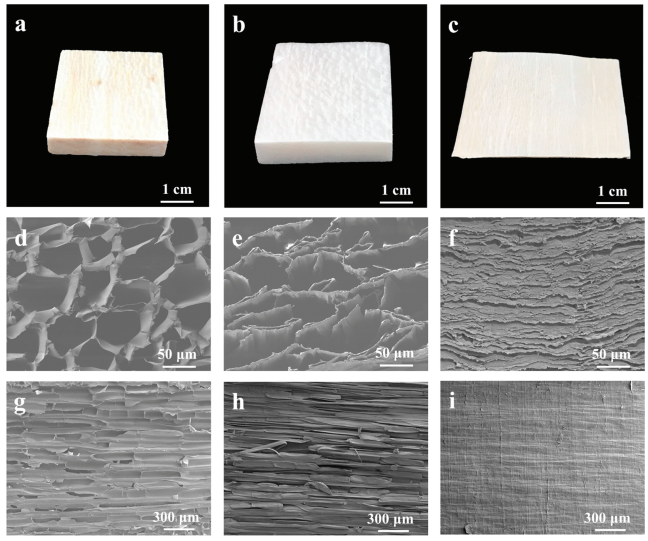

Fig. 3. Structural characterization of the NW, WA and $CWA_{18\%}$. (a) Photo of the NW. FE-SEM images of the NW: (d) transverse section image; (g) tangential section image. (b) Photo of the WA. FE-SEM images of the WA: (e) transverse section image; (h) tangential section image. (c) Photo of the $CWA_{18\%}$. FE-SEM images of the $CWA_{18\%}$: (f) transverse section image; (i) tangential section image.

completely white after delignification, supposing the almost all lignin and hemicellulose have been removed. Above hypothesis has been proved by component analysis (Fig. 2a) and It also suggested the WA consisting of almost whole cellulose has been successfully fabricated. After having 18% MC, the WA was directly compressed into hard cellulosic slice (Fig. 3c). The SEM images showed the NW possesses a three-dimensional (3D) porous structure with lumina of 30–50 μm in diameter and 150–400 μm in length (Figs. 3d and g). After delignification and freeze-drying, the intrinsic cell lumina structure was destroyed and the connection among wood cells was also broken (Fig. 3e). Besides, the tangential section SEM image of WA showed that the original tracheid structure has almost disappeared (Fig. 3h). After compression, wood cells had been stacked together to form layer-by-layer architecture liking nacre structure. And in every layer, cellulose nanofibers and cell walls had entangled tightly and merged together by compression (Fig. 3f). Meanwhile, the tangential SEM images of $CWA_{18\%}$ indicated the structure of every layer is dense and compact (Fig. 3i).

Fig. 4 displays the tensile stress-strain curves (Fig. 4a) and corresponding mechanical properties of NW, WA and CWAs. Because of the fluffy and fragile characteristic formed during freeze-drying, the tensile strength and failure strain of WA cannot be tested. The compressed wood aerogels compressed under 9% moisture content ($CWA_{9\%}$) has an improved mechanical performance compared to NW (tensile strength of 47.54 *vs.* 23.22 MPa, and Young's modulus of 13.14 *vs.* 2.82 GPa) (Fig. 4b), which can be ascribed to the water molecules-induced hydrogen bonding between cellulose nanofibers. Above results implied that the dense structure initiated by hydrogen bonding endowed $CWA_{9\%}$ with a big mechanical performance. The toughness of the $CWA_{9\%}$ is also 8 times than that of NW, reaching 1.6 MJ/m^3. With the increase of MC to 18%, the CWA showed sharply and simultaneously enhanced mechanical properties as compared to NW (tensile strength of 135.63 *vs.* 23.22 MPa, Young's modulus of 18.68 *vs.* 1.82 GPa, and toughness of 1.6 *vs.* 0.16 MJ/m^3) (Fig. 4b), which is 5.8 times for tensile strength, 10.3 times for Young's modulus, and 10 times for toughness. Above results indicated that the WA contains a lot of binding sites that can form hydrogen bonding with water molecules and 9% MC has not saturated the binding sites in the WAs. That means the 9% MC is lower than fiber saturation point of WAs sample. As the MC increased to 18%, more water molecules were adsorbed and formed hydrogen bonding with O and H atoms of cellulose nanofibers. So, the $CWA_{18\%}$ sample has a bigger mechanical property than $CWA_{9\%}$. Besides, the $CWA_{18\%}$ also showed very high specific strength (161.46 MPa cm^3/g) as compared to other conventional building materials, including concrete, low carbon steel (AISI 1010, LCS), stainless steel (304, SS), and aluminum alloy (7075-T6, AA). This high specific strength is because of the relatively low density of the cellulosic materials, making the compressed wood aerogel a light yet strong material.

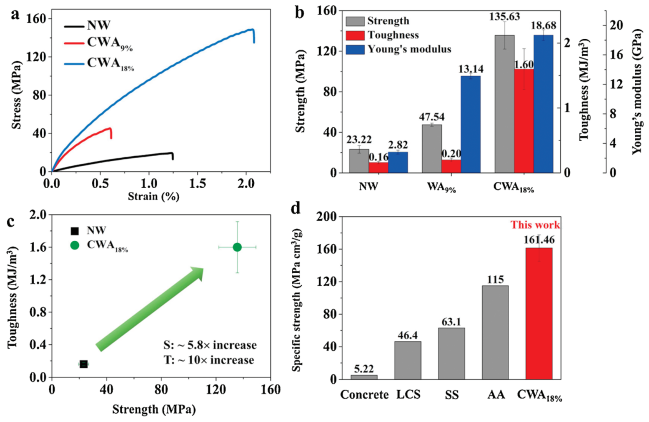

Fig. 4. Mechanical properties of NW and CWA compressed at different moisture content (MC 0%, 9% and 18%). (a) Typical tensile stress-strain curves, (b) the respective tensile strength, toughness, and Young's modulus values derived from the tensile stress-strain curves, (c) the comparation of the toughness and strength of NW and $CWA_{18\%}$, (d) Comparison of the specific strength of $CWA_{18\%}$ and other conventional building materials, including concrete, low carbon steel (AISI 1010, LCS), stainless steel (304, SS), and aluminium alloy (7075-T6, AA).

The essential cause of the increased densification, compactness, and mechanical properties at higher MC could be analyzed in three aspects. Firstly, water molecule can be viewed as flexibilizer and softener to WAs, causing cell walls and its internal cellulose nanofibers to densely pack together and tightly intertwine under compression. Secondly, 0%, 9% and 18% MCs are all lower than the fiber saturation point of WAs. So, there are more bound water in cellulose nanofibers, more hydrogen bonding between cellulose nanofibers, and less internal defect in the structure of $CWA_{18\%}$. Thirdly, there is a sliding movement between cellulose nanofibers in the tensile test process, leading to the break of hydrogen bonding between cellulose nanofibers. However, the broken hydrogen bonding can quickly regenerate due to water-molecule bridging effect [34]. In addition, the cellulose nanofibers intertwined together under compression, giving CWA a good fracture toughness [35]. Thus, the more MCs gave CWA more hydrogen bonding, faster regeneration, and good fracture toughness. Based on the above reasons, the compressed wood aerogel at 18% MC has a stronger tensile strength and a longer strain under tensile stress test, inducing a bigger toughness.

Because our final product was from the WA, we have also characterized a typical property of WA - the thermal insulation performance. As shown in Fig. S1a (Supporting information), the thermal conductivity of the WA is smaller than that of NW (0.044 *vs.* 0.039 W/mK), indicating delignification and freeze drying can increase the porosity of sample and then endowing superior thermal insulation property of WA. Comparing to the NW and WA, the $CWA_{18\%}$ sample has a bigger thermal conductivity. Due to the compression, the wood cellulose nanofibers were tightly entangled together and the porosity of sample was reduced, inducing the increase of the thermal conductivity (up to 0.102 W/mK). This trend is also consistent with the density, porosity, and microstructure as shown in the previous section. Although the $CWA_{18\%}$ has a relative bigger thermal conductivity, the value is still much smaller than some traditional commercial building materials (Fig. S1b in Supporting information). Together with the mechanical property characterization, we actually fabricated a kind of engineering materials with superior mechanical performance and thermal insulation property.

In summary, we fabricated a lightweight, strong and tough cellulosic structural material by three-step streamlined process, including making WA, rehydration and water molecule-induced hydrogen-bonding assembling under compression. The obtained WAs showed a low thermal conductivity of 0.039 W/mK along the layer-stacking direction, closing to a pure cellulose-based aerogel. In addition, the CWAs showed an increased mechanical property along the increased MC prior to compression. Surprisingly, the $CWA_{18\%}$ had a highest tensile strength of 135.63 MPa and toughness of 1.60 MJ/m^3, which are approximately 6 and 10 times higher, respectively, as compared to those of NW. More importantly, there's a simultaneously improved strength and toughness in CWAs, and the reinforcement mechanism was analyzed. Because of the top-down fabrication, sustainable materials and superior mechanical properties, the high-performance cellulosic material can be used in modern architecture, new energy vehicles, *etc.* Besides, this preparation process also provided the sustainable solution of reusing the wasted WAs.

Declaration of competing interest

The authors report no declarations of interest.

Acknowledgements

We acknowledge the support of the National Natural Science Foundation of China (No. 51803093) and National Science Foundation of Jiangsu Province (No. BK20180770).

Appendix A. Supplementary data

Supplementary material related to this article can be found, in the online version, at doi:https://doi.org/10.1016/j.cclet.2021.03.044.

References

[1] R.O. Ritchie, Nat. Mater. 10 (2011) 817–822.
[2] W. Cui, M.Z. Li, J.Y. Liu, et al., ACS Nano 8 (2014) 9511–9517.
[3] Y.P. Feng, L.P. Ding, D.Y. Ji, L.L. Wang, W. Guo, Chin. Chem. Lett. 29 (2018) 892–894.
[4] W. Li, J. Liu, B. Liang, Y. Shu, J. Wang, Compos. Part B: Eng. 204 (2021) 108492.
[5] Y.X. Liu, S.H. Yu, L. Bergstrom, Adv. Funct. Mater. 28 (2018) 1703277.
[6] P. Xu, T. Erdem, E. Eiser, Soft Matter 16 (2020) 5497–5505.
[7] Y. Wang, T. Li, P.M. Ma, et al., ACS Nano 12 (2018) 6228–6235.
[8] H.L. Gao, S.M. Chen, L.B. Mao, et al., Nat. Commun. 8 (2017) 287.
[9] Y.P. Chen, B.K. Dang, C.D. Jin, Q.F. Sun, ACS Nano 13 (2019) 371–376.
[10] Y.P. Chen, J.Z. Fu, B.K. Dang, et al., ACS Nano 14 (2020) 2036–2043.
[11] Y. Zou, P. Yang, L. Yang, et al., Polymer 217 (2021) 123464.
[12] L. Chen, Z. Xu, F. Wang, et al., Compos. Commun. 20 (2020) 100355.
[13] F. Wang, J.Y. Cheong, Q. He, et al., Chem. Eng. J. 414 (2021) 128767.
[14] C. Wang, Z. Yang, X. Wang, Q. Yu, J. For. Eng. 4 (2019) 10–18.
[15] B. Joseph, S.V. K, C. Sabu, N. Kalarikkal, S. Thomas, J. Bioresour. Bioprod. 5 (2020) 223–237.
[16] X.S. Han, R. Bi, H. Oguzlu, ACS Sustain. Chem. Eng. 8 (2020) 14955–14963.
[17] M.Y. Li, S.C. Cheng, D. Li, et al., Chin. Chem. Lett. 26 (2015) 221–225.
[18] D.W. Wei, H. Wei, A.C. Gauthier, et al., J. Bioresour. Bioprod. 5 (2020) 1–15.
[19] F. Xu, Y. Chen, T. You, J. Mao, X. Zhang, J. For. Eng. 4 (2019) 1–7.
[20] X.S. Han, Y.H. Ye, F. Lam, J.W. Pu, F. Jiang, J. Mater. Chem. A 7 (2019) 27023–27031.
[21] Q.Q. Mei, X.J. Shen, H.Z. Liu, B.X. Han, Chin. Chem. Lett. 30 (2019) 15–24.
[22] B. Thomas, M.C. Raj, K.B. Athira, et al., Chem. Rev. 118 (2018) 11575–11625.
[23] R.J. Moon, A. Martini, J. Nairn, J. Simonsen, J. Youngblood, Chem. Soc. Rev. 40 (2011) 3941–3994.
[24] H.L. Zhu, S.Z. Zhu, Z. Jia, et al., Proc. Natl. Acad. Sci. U. S. A. 112 (2015) 8971–8976.
[25] W.T. Cao, F.F. Chen, Y.J. Zhu, et al., ACS Nano 12 (2018) 4583–4593.
[26] L. Chang, Z. Peng, T. Zhang, C. Yu, W. Zhong, Nanoscale 13 (2021) 3079–3091.
[27] S.K. Biswas, H. Sano, M.I. Shams, H. Yano, ACS Appl. Mater. Inter. 9 (2017) 30177–30184.
[28] Q.H. Tang, L. Fang, Y.F. Wang, M. Zou, W.J. Guo, Nanoscale 10 (2018) 4344–4353.
[29] R.Y. Mi, T. Li, D. Dalgo, et al., Adv. Funct. Mater. 30 (2020) 1907511.
[30] O.C. Compton, S.W. Cranford, K.W. Putz, et al., ACS Nano 6 (2012) 2008–2019.
[31] Q. Zhang, T. Li, A. Duan, et al., J. Am. Chem. Soc. 141 (2019) 8058–8063.
[32] M. Frey, D. Widner, J.S. Segmehl, et al., ACS Appl. Mater. Inter. 10 (2018) 5030–5037.
[33] Y. Hou, Q.F. Guan, J. Xia, et al., ACS Nano 15 (2021) 1310–1320.
[34] Y.B. Zhou, C.J. Chen, S.Z. Zhu, et al., Mater. Today 30 (2019) 17–25.
[35] T. Li, C.J. Chen, A.H. Brozena, et al., Nature 590 (2021) 47–56.